Available online at www.sciencedirect.com
ScienceDirect
Spectrochimica Acta Part A 70 (2008) 177–186
SPECTROCHIMICA ACTA PART A
www.elsevier.com/locate/saa

The electronic absorption spectra of some acyl azides Molecular orbital treatment

Rafie H. Abu-Eittah*, Adel A. Mohamed, A.M. Farag, Ahmed M. Al Omar

Department of Chemistry, Faculty of Science, University of Cairo, Giza, Egypt

Received 7 June 2005; received in revised form 22 March 2007; accepted 18 May 2007

Abstract

The electronic absorption spectra of benzoyl azide and its derivatives: *p*-methyl, *p*-methoxy, *p*-chloro and *p*-nitrobenzoyl azide were investigated in different solvents. The observed spectra differ basically from the electronic spectra of aryl azides or alkyl azides. Four intense π–π^* transitions were observed in the accessible UV region of the spectrum of each of the studied compounds. The contribution of charge transfer configurations to the observed transitions is rather weak. Shift of band maximum with solvent polarity is minute. On the other hand, band intensity is highly dependent on the solvent used. The observed transitions are delocalized rather than localized ones as in the case with aryl and alkyl azides. The attachment of the C═O group to the azide group in acyl azides has a significant effect on the electronic structure of the molecule. The arrangements as well as energies of the molecular orbitals are different in acyl azides from those in aryl azides. The first electronic transition in phenyl azide is at 276 nm, whereas that of bezoyle azide is at 251 nm.

Ab initio molecular orbital calculations using both RHF/6-311G* and B3LYP/6-31+G* levels were carried out on the ground states of the studied compounds. The wave functions of the excited states were calculated using the CIS and the AM1-CI procedures.

Keywords: Acyl azides; Spectra of acyl azides; Molecular orbital calculations of acyl azides; Specrta and molecular orbital calculations of acyl azides

1. Introduction

The biological activities of aroyl azides and nicotinic azides are wide and are the subject of extensive investigations. For instance, *p*-chloro and *o*-chloro azides are used in fungal metabolites and have antimicrobial activities [1,2] whereas nicotinic and isonicotinic azides have some pharmacological effects [3]. Benzoyl azide and nicotinic azide caused powerfully effective hypotension, hematuria and cardiac irregularities in rabbits without visible toxicity at doses of 10 mg/Kg by mouth [4].

The effect of substituent on the electronic absorption spectra of a related series of benzyl azide derivatives, $RC_6H_4CON_3$ (R = *p*-OCH_3, *p* = Br, H, *m*-NO_2 and *p*-NO_2) were studied [5,6]. The values of λ_{max} increase substantially when R is an electron donating group in the *para* position. However, with R = NO_2, the values of λ_{max} are at about the same values of nitrobenzene and *p*-nitro benzoic acid, that is, the azido group acts as an electron withdrawing group. It has been found that halogens can act as electron donating or withdrawing groups depending on the nature of other substituent [7]. The values of band maxima are quite sensitive to the substituent effects and vary systematically with substituent constant [5].

The electronic structures of *p*-benzoyl azide derivatives, $RC_6H_4CON_3$, R = H, F, Cl, Br and I, were calculated using the PPP-method and CI among all singly excited configurations. Absorption bands in the near UV region were assigned to three electronic transitions: two of which are due to local excitations in the phenyl group and the other is a local excitation in the azide group [8].

While the absorption spectrum of alkyl azides is that of the isolated azide group, the spectra of aromatic azides are essentially those of the parent hydrocarbons, only a weak additional band due to azido group appears as a shoulder on the long wavelength side of the hydrocarbon spectrum [9]. The coupling effect of the azido group with the aromatic system corresponds to a charge flow from nitrogen towards the ring (the azido group is an electron donating with a Hammett constant $\sigma_p^+ = -0.54$) [10]. This lowers the energy of the non-bonding π_y^n – orbital below the level of $\sigma(sp^2)$-orbital; consequently, the lowest energy transition, namely $\sigma(sp^2) \rightarrow \pi_y^*$, where the π_y^* orbital extends now over the whole aromatic system.

---

* Corresponding author.
E-mail address: abueittah@chem-sci.cu.edu.eg (R.H. Abu-Eittah).

1386-1425/$ – see front matter © 2007 Published by Elsevier B.V.
doi:10.1016/j.saa.2007.05.066

In this work, the electronic absorption spectra of: benzoyl azide, *p*-methyl, *p*-methoxy, *p*-chloro, and *p*-nitrobenzoyl azides have been investigated using different solvents. Gaussian analysis was used to analyze the observed spectra.

2. Experimental

2.1. Solvents

Ethanol, methanol, acetonitrile, dichloromethane, heptane, hexane cyclohexane and diethyl ether are all Merck AR-reagents and used without further purification.

2.2. Compounds

All compounds were prepared by the methods reported in the literature [11]. The benzoyl azides were prepared by the action of sodium nitrite on the corresponding hydrazide in aqueous hydrochloric acid with stirring at −5 °C using sodium chloride-ice bath. Stirring continued for 30 min at the same temperature, and then ether is added. The ethereal layer is separated, washed several times with cold dilute solution of sodium carbonate, then dried over anhydrous sodium sulphate. Ether was removed under reduced pressure and the product was purified by crystallization from dry ether. IR-spectra were performed to confirm the purity of the product. The compounds prepared: benzoyl azide, m.p. = 27 °C (reported value [12] is 26 °C), *p*-methylbenzoyl azide: m.p. = 35.5 °C (reported value [13] is 35.0 °C), *p*-methoxybenzoyl azide: m.p. = 69–70 °C (reported is 70–71 °C [14]), *p*-chlorobenzoyl azide: m.p. = 42 °C (reported [15] is 43 °C)$^{(81)}$, *p*-nitrobenzoyl azide: m.p. = 64 °C (reported [16] is 65 °C).

2.3. Apparatus

The spectral measurements were performed on a Perkin-Elmer Lambda 4B UV–vis spectrophotometer using 1.0 cc fused silica cells.

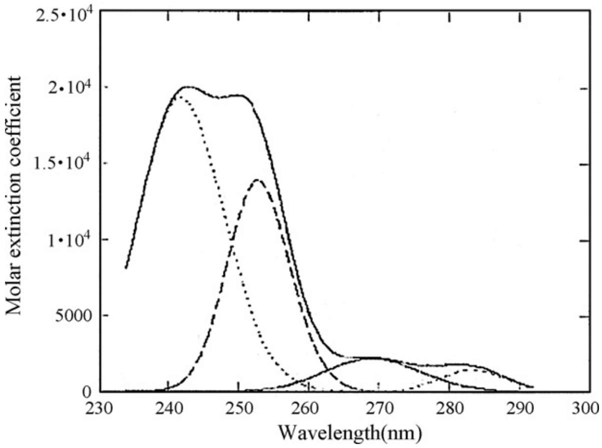

Fig. 1. Electronic absorption spectra of benzoyl azide in heptane and its Gaussian analysis.

3. Method of calculation

Ab initio molecular orbital calculations were carried out using the RHF level with 6-31+G* basis set. The molecules were fully optimized without any constrains. Effect of electron correlation on the ground state properties was considered by applying the DFT method as given by the B3LYP/6-31+G* procedures. The wave functions of the excited states and their energies were calculated using both ab-initio CIS and the semiemperical AM1-CI methods.

All calculations were carried out using the free distributed GAMESS 6.4 program [17] and a MOPAC package [18].

Gaussian analysis of the spectra was performed using a MATHCAD PLUS package [19].

4. Results and discussion

4.1. Electronic absorption spectra

4.1.1. Benzoyl, p-methylbenzoyl and p-methoxybenzoyl azides

Fig. 1 shows the absorption spectra of benzoyl azide in heptane as a solvent. Gaussian analysis of the spectrum in heptane, using a MATHCAD PLUS package [19] indicates the existence of four electronic transitions in the accessible UV region. Band maximum and molar extinction coefficient are given in Table 1. The spectra of benzoyl azide have been investigated in different solvents. There is a small shift in band maximum with solvent polarity a result which means a minor contribution of charge transfer configurations to the excited states of the molecule and that there is no detectable change in the polarity of the molecule on electronic excitation. On the other hand, band intensity varies significantly with the type of the solvent. This *is due* to the fact that acyl azides are stronger dipoles than the corresponding aryl *azides*. Benzoyl azide has a dipole moment $\mu = 2.60$D whereas that of phenyl azide is 1.44 [20]. The values of the molar extinction coefficients of the observed transitions of benzoyl azide, using heptane as a solvent, vary between 1150 ($\lambda_{max} = 284$) to 19,330 ($\lambda_{max} = 241$) a result which indicates that all of the observed bands are due to $\pi \rightarrow \pi^*$ localized transitions.

The spectra of the studied acyl azides are of interest because they identify the excited states which arise on light absorption and are potentially involved in photolytic reaction. In the acyl azides, conjugation with the carbonyl group causes a small blue shift of the low energy band and a slight enhancement of its intensity as compared to aryl azides. The flow of charge from azide group to aryl group in aryl azides is inhibited in acyl azides as a result of the presence of the carbonyl group and this leads to the inhibition of the perturbation effect of the azide group on the spectra of the aryl ring in acyl azides. The contribution of charge transfer configurations to the excited states is small. The perturbation effect of the $-CON_3$ on the spectra of the aryl ring has to be considered on examining the spectra of acyl azides. The spectra of acyl azides are different from those of aryl azides and cannot be assigned to those of isolated azide or aryl groups as in the case of aryl azides. Molecular orbital calculations will confirm this conclusion.

Table 1
Band maxima (λ_{max}, nm), molar extinction coefficients(ε, mol^{-1} L cm^{-1}), and oscillator strengths of benzoyl azide, *p*-methyl azide and *p*-methoxybenzoyl azide in different solvents

Solvent	Benzoyl azide			*p*-Methylbenzoyl azide			*p*-Methoxybenzoyl azide		
	λ_{max}	ε	*f*	λ_{max}	ε	*f*	λ_{max}	ε	*f*
Heptane	241	19370	0.219	250	17120	0.164	212	15770	0.149
	252	12940	0.097	260	14390	0.129	221	14200	0.141
	269	2160	0.028	275	3220	0.022	254	6500	0.119
	284	1150	0.007	286	1980	0.014	271	22000	0.312
							284	12970	0.079
Diethyl ether	242	16140	0.163	251	17200	0.200	–	–	–
	253	11580	0.128	262	15900	0.158	255	7500	0.132
	270	2000	0.023	276	2610	0.026	272	17990	0.248
	285	1660	0.011	285	1480	0.015	286	17450	0.187
Acetonitrile	243	14340	0.189	253	19000	0.221	215	13460	0.227
	254	12580	0.137	263	16500	0.177	223	39320	0.072
	271	2100	0.021	277	3210	0.032	255	5900	0.104
	285	1350	0.011	286	1580	0.016	273	16890	0.246
							289	17360	0.209
Ethanol	244	13240	0.163	253	19200	0.223	215	13570	0.229
	255	11880	0.128	264	17000	0.189	224	5000	0.088
	271	2000	0.023	277	3410	0.034	256	5700	0.100
	285	1350	0.011	286	2180	0.022	274	16900	0.246
							290	18450	0.222
Dichloro-methane	245	13350	0.173	254	17000	0.198	–	–	–
	256	11800	0.126	265	15600	0.162	256	5740	0.101
	272	2050	0.025	277	3410	0.034	274	14330	0.219
	285	1380	0.011	286	2180	0.022	290	16000	0.210

Figs. 2 and 3 show the electronic absorption spectra of *p*- and *o*-methylbenzoyl azide. Methyl substitution facilitates charge transfer transitions and one observes a red shift of band maximum in polar solvents, Table 1. The intensity of the observed bands, $19200 > \epsilon > 1900$, indicates that they correspond to $\pi \rightarrow \pi^*$ transitions. Band maxima of *p*-methylbenzoyl azide are slightly red shifted: $\lambda_{max} = 250$, 260, 275 and 286 nm compared to those of benzoyl azide: $\lambda_{max} = 241$, 252, 269 and 284 nm as a result of the inductive effect of the $-CH_3$ group.

Methoxy substitution causes a detectable perturbation effect, as a result five intense electronic transitions are obtained, Figs. 4 and 5; the spectrum of *p*-methoxybenzoyl azide, Fig. 4 and Table 1. Variation of band maximum with solvent polarity is minor, hence a minor change in polarity is experienced on excitation. Bhaskar [5] studied the effect of substituent on the electronic absorption spectra of thiocarbanilide, benzyl azide, diphenylcarbodiimide and acetophenone. The values of band maximum, in the case of benzyl azide, increases appreciably when an electron donating substituent as $-OCH_3$ is present. However, the electron withdrawing nitro group leads to band

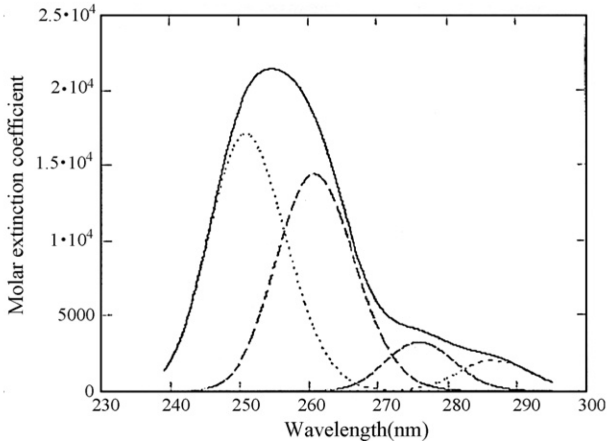

Fig. 2. Electronic absorption spectra of *p*-methylbenzoyl azide in heptane and its Gaussian analysis.

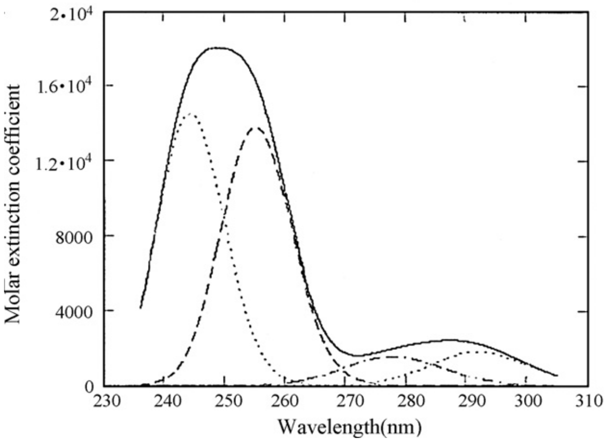

Fig. 3. Electronic absorption spectra of *o*-methylbenzoyl azide in heptane and its Gaussian analysis.

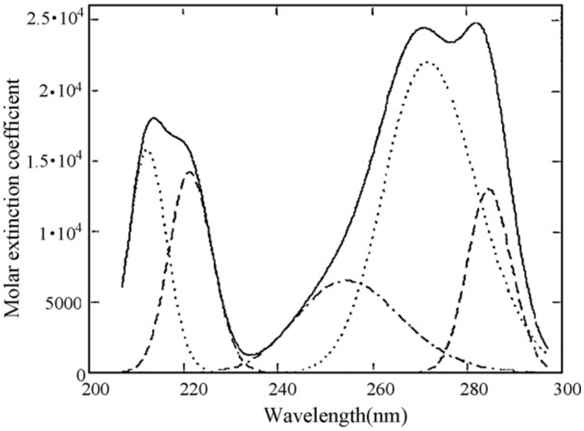

Fig. 4. Electronic absorption spectra of *p*-methoxybenzoyl azide in heptane and its Gaussian analysis.

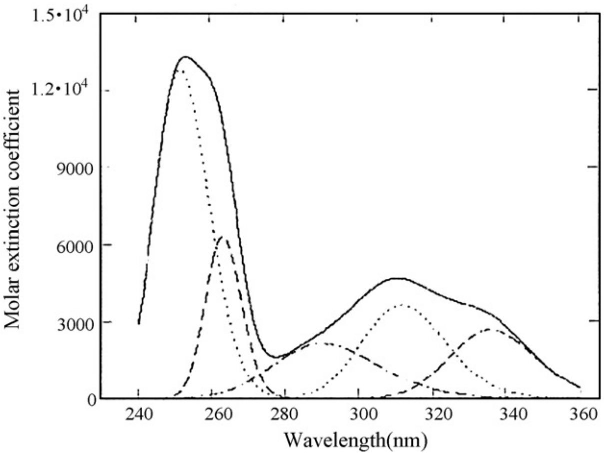

Fig. 5. Electronic absorption spectra of *o*-methoxybcnzoyt azide in heptane and its Gaussian analysis.

maximum at the same value as that of nitrobenzene. This result shows that the acid azido group is an electron withdrawing group.

4.1.2. *p-Chlorobenzoyl and p-nitrobenzoyl azides*

The spectra of *p*- and *o*-chlorobenzoyl azides show four electronic transitions in the 240–300 nm region, Figs. 6 and 7 corresponding to $\pi \rightarrow \pi^*$ but with band maxima that differ significantly from those of benzoyl, *p*-CH_3 and *p*-OCH_3 benzoyl azides (Table 2). All transitions are red shifted in *p*-chlorobenzoyl azide as compared to those in benzoyl, *p*-CH_3 or *p*-OCH_3 benzoyl azides. The highest energy transition appears at 252 nm in *p*-chlorobenzoyl azide compared to 241 nm in benzoyl azide.

Substitution by a nitro group causes the strongest perturbation effect on the parent nucleus. The spectra of *p*-NO_2 benzoyl azide are shown in Fig. 5. Four intense $\pi \rightarrow \pi^*$ transitions are observed with band maxima (Table 2) that differ significantly from the previously studied compounds. Both the $-NO_2$ and $-CON_3$ groups inhibit the electronic effect of each other, hence, the contribution of the charge transfer configurations to the electronic states is minimum.

4.2. *Molecular orbital calculations*

4.2.1. *Benzoyl azide*

The rotation of the azide group around the C–N single bond results in two conformers of benzoyl azide. The most stable

Table 2
Band maxima (λ_{max}, nm), molar extinction coefficients (ε, $mol^{-1}\,L\,cm^{-1}$), and oscillator strengths of benzoyl azide, *p*-methyl azide and *p*-methoxybenzoyl azide in different solvents

Solvent	*p*-Chlorobenzoyl azide			*p*-Nitrobenzoyl azide		
	λ_{max}	ε	f	λ_{max}	ε	f
Heptane	252	21800	0.169	253	13700	0.167
	263	17400	0.123	266	11000	0.128
	274	3320	0.023	290	2100	0.025
	286	1780	0.013	309	780	0.007
Diethyl ether	254	20090	0.194	254	21800	0.267
	263	15300	0.117	266	18000	0.211
	274	3220	0.022	290	3410	0.040
	286	1780	0.013	309	1010	0.010
Acetonitrile	254	18700	0.195	257	15400	0.191
	264	14300	0.143	270	12200	0.143
	275	2660	0.024	293	3200	0.038
	286	1880	0.017	311	1080	0.010
Ethanol	254	24300	0.255	256	18000	0.225
	264	19300	0.194	269	15200	0.178
	276	3510	0.032	292	3090	0.046
	286	2180	0.020	310	1480	0.014
Dichloro-methane	256	16700	0.174	259	18500	0.230
	265	13900	0.138	272	15300	0.179
	276	3510	0.027	294	3600	0.043
	286	2180	0.020	311	1180	0.011

Table 3
Structural properties of the ground state of the studied benzoyl azide and its derivatives using the RHF/6-311G* and (B3LYP/6-31+G*) methods

Property	Benzoyl azide	*p*-CH_3 benzoyl	*p*-OCH_3 benzoyl	*p*-Cl benzoyl	*p*-NO_2 benzoyl
Total energy (a.u.)	−506.2494 −506.2016[a] *−506.1886*[b]	−545.2942 −548.1946 *−548.5081*	−620.1573 −623.7509 *−623.7176*	−965.1749 −968.7968 *−968.7833*	−709.7710 −713.7083 *−713.6947*
Dipole moment (D)	2.19 [2.60][c]	2.625	3.805	1.550	4.257
Total bond order					
C_1—C_6 (*ring*)	1.030	1.036	1.096	1.024	1.013
C_1—O_5	1.965	1.965	1.961	1.968	1.973
C_1—N_2	1.046	1.042	1.097	1.053	1.065
N_2—N_3	1.109	1.010	1.117	1.104	1.093
N_3—N_4	2.389	2.388	2.385	2.392	2.398
Charge density					
C_1	+0.614	+0.612	+0.615	+0.617	+0.420
N_2	−0.487	−0.488	−0.491	−0.486	−0.485
N_3	+0.411	+0.412	+0.412	+0.410	+0.410
N_4	−0.062	−0.066	−0.068	−0.058	−0.044
O_5	−0.465	−0.458	−0.471	−0.462	−0.453
C_6H_5	−0.011	0.048	+0.200	+0.045	+0.322
Energy					
HOMO (a.u.)	−0.34770	−0.33720	−0.32480	−0.3619	−0.3770
LUMO (a.u.)	+0.07420	+0.07780	+0.08510	+0.0634	+0.0240

[a] Conformer A.
[b] Conformer B.
[c] Experimental dipole moment.

conformer (A) is planer and is of lower energy, 0.013 a.u. than the non planer one (B) at the B3LYP/6-31+G* level, Table 3.

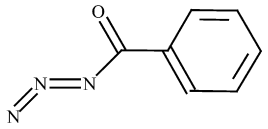

(A)

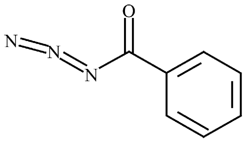

(B)

Conformer (A) will be used for all coming calculations. The optimized geometry of benzoyl azide is calculated using the RHF/6-311G* and B3LYP/6-31+G* methods, results are given in Tables 3 and 4. The calculated dipole moment is 2.19 D and agrees satisfactorily with the experimental value, 2.60D [20]. Comparing the results of both levels shows that the DFT elongates the C—O, C—N and N—N bonds with maximum error of 0.03 Å, while the difference in case of bond angles is only 1°. The RHF results in Table 3 lead to some important predictions, the C_1—C_6 bond length is 1.488 Å compared to 1.554 Å for a typical C—C single bond which indicates a weak π-overlap between the benzene ring and the —C=O carbon. Along the same line, C_1—C_6 bond order is 1.030, which is slightly larger than that between singly bonded C—C atoms. The bond length C_1—N_2 is 1.402 Å compared to 1.472 Å for a pure single C—N bond and 1.287Å for a pure C—N double bond. Thus in benzoyl azide the C—N bond

Table 4
Parameters of the equilibrium geometry of the ground state of benzoyl azide and its derivatives using the RHF/6-311G* and (B3LYP/6-31+G*) methods

Parameters	Benzoyl azide	*p*-CH_3	*p*-OCH_3	*p*-Cl	*p*-NO_2
Bond length					
r-(C_1—C_6) (Å)	1.488 (1.485)	1.485 (1.402)	1.481 (1.475)	1.488 (1.483)	1.496 (1.491)
r-(C_1—O_5)	1.197 (1.218)	1.190 (1.218)	1.191 (1.220)	1.188 (1.218)	1.188 (1.217)
r-(C_1—N_2)	1.402 (1.435)	1.403 (1.436)	1.405 (1.439)	1.399 (1.433)	1.394 (1.427)
r-(N_2—N_3)	1.259 (1.247)	1.254 (1.246)	1.253 (1.246)	1.256 (1.248)	1.260 (1.250)
r-(N_3—N_4)	1.088 (1.133)	1.082 (1.132)	1.082 (1.133)	1.081 (1.131)	1.080 (1.130)
Bond angle					
$\theta(O_5C_1N_2)$ (°)	123.64 (124.70)	123.02 (124.56)	123.80 (125.00)	123.40 (124.57)	123.94 (124.10)
$\theta(C_6C_1N_2)$	113.20 (112.7)	113.27 (112.66)	113.21 (112.7)	113.07 (112.60)	112.97 (112.6)
$\theta(C_1N_2N_3)$	111.23 (114.4)	111.30 (114.431)	111.31 (114.3)	111.24 (114.40)	111.22 (114.4)
$\theta(N_2N_3N_4)$	175.30 (174.7)	175.27 (174.678)	175.35 (174.8)	175.26 (174.60)	175.17 (174.4)
$\theta(C_7C_6C_1)$	117.60 (117.9)	117.92 (118.115)	118.01 (118.3)	122.86 (118.00)	122.24 (117.7)
$\theta(N_4N_3N_2C_1)^0$	180.0 (180.0)	180.0 (180.0)	180.0 (180.0)	180.0 (180.0)	180.0 (180.0)
$\theta(C_6C_1N_2N_3)^0$	180.0 (180.0)	180.0 (180.0)	180.0 (180.0)	180.0 (180.0)	180.0 (180.0)

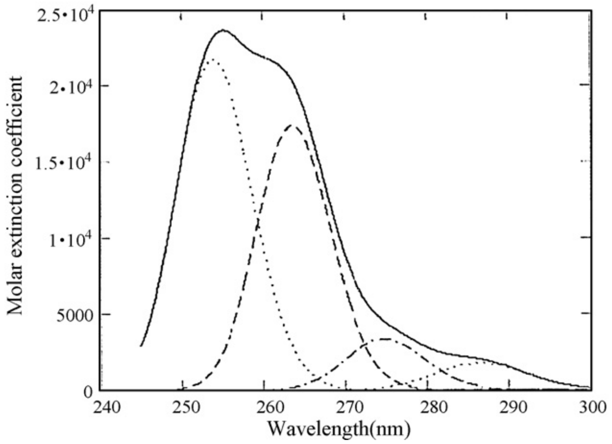

Fig. 6. Electronic absorption spectra of *p*-chlorobenzoyl azide in heptane and its Gaussian analysis.

is essentially a single bond, the bond order is 1.046. The bond length N(2)–N(3) is 1.255 Å compared with 1.240 Å for N–N double bond and 1.400 Å for pure N–N single bond and 1.100 for N–N triple bond. Hence, in benzoyl azide, N(2)–N(3) bond is essentially a double bond. On the other hand, the N(3)–N(4) bond length is 1.081 Å reflecting a nice triple bond character with a bond order of 2.389. The above results lead to two resonating structures (c) and (d) for benzoyl azide, structure (c) is favored for the ground state.

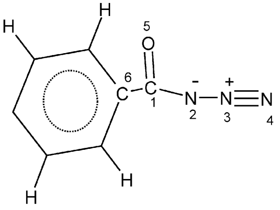

c

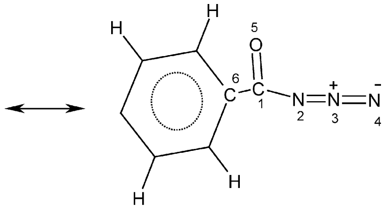

d

The distribution of charge density is calculated and shown in Table 3. The bond angle, $\theta(N_2N_3N_4)$ is 175.30° in the optimized geometry of benzoyl azide, hence a slight bent structure is assigned to the azide group and indicating the contribution of conformer (a). However, the dihedral angle $\theta(N_3N_4N_2C_1)$ between the plane of the azide group and that of C_6H_5CO is ∼180° indicating a planar configuration of the molecule.

The optimized geometry of benzoyl azide at both levels was used as an entry to calculate the excited states of the molecule

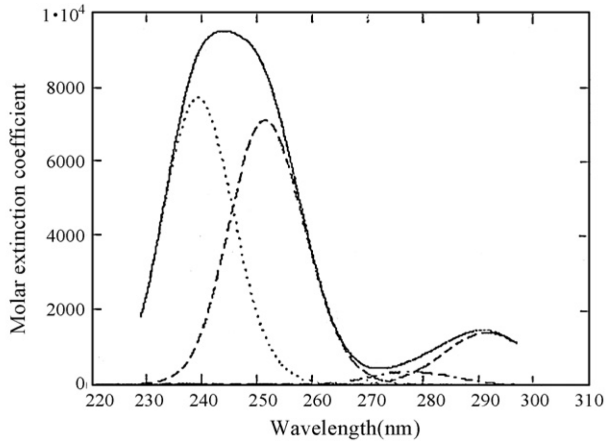

Fig. 7. Electronic absorption spectra of *o*-chlorobenzoyl azide in heptane and its Gaussian analysis.

Table 5
Transition energies (eV) calculated at the ab initio, CIS/B3LYP/6-341+G* and the semi-empirical AM1/6-311G*levels

Compound	CIS/B3LYP/6-31+G*	AM1/6-311G*	Exp.
Benzoyl azide	5.158	4.45	4.37
	5.669	4.65	4.61
	5.853	5.00	4.92
	5.918	5.50	5.15
p-Cl	5.938	4.38	4.34
	5.999	4.58	4.53
	6.006	4.64	4.71
	6.010	5.28	4.92
p-Me	5.693	4.41	4.34
	5.805	4.50	4.51
	5.843	4.90	4.77
		5.33	4.96
p-MeO	5.990	4.28	4.37
	6.203	4.40	4.58
		5.09	4.89
		5.53	5.61
		5.80	5.81
p-NO_2	5.641	4.20	4.01
	5.695	4.43	4.28
	5.846	4.77	4.68
	5.883	5.21	4.90

For the studied compounds.

Table 6
The weight percent of the atomic orbitals in the wave functions of molecular orbitals Ψ_{25}–Ψ_{30} of the different chromophores of the studied benzoyl azides

MO	wt.%					
	ψ_{25}, π_1	ψ_{26}, π_2	ψ_{27}, π_3	ψ_{28}, π_1^*	ψ_{29}, σ^*	ψ_{30}, π_2^*
Chromophore benzoyl azide						
$-N_3$	79	8	1	23	86	56
$-CO$	18	3	1	32	10	1
C_6H_5-	1	89	98	55	4	43
p-Methylbenzoyl azide						
$-N_3$	83	1	5	48	94	45
$-CO$	14	1	2	24	5	1
p-$CH_3C_6H_4-$	3	98	93	28	1	54
p-Methoxybenzoyl azide						
$-N_3$	82	1	2	26	90	4
$-CO$	17	1	3	30	8	1
p-$CH_3OC_6H_4-$	1	98	95	44	2	95
p-Chlorobenzoyl azide						
$-N_3$	81	1	3	20	90	55
$-CO$	17	1	2	25	9	4
p-ClC_6H_4-	2	98	95	55	1	41
p-Nitrobenzoyl azide						
$-N_3$	21	8	61	4	94	70
$-CO$	13	1	4	9	3	13
p-$NO_2C_6H_4-$	66	91	35	87	3	17

Table 7
CI wave functions of the excited states and the corresponding transition energies (ΔE) of benzoyl azide

State functions	Assignment	ΔE (eV)	
		Calc.	Obs.
$\Psi_{\mathrm{EX\,I}} = \pm 0.18\phi_{27}^{-1}\phi_{28} \pm 0.47\phi_{26}^{-1}\phi_{28} \pm 0.37\phi_{25}^{-1}\phi_{28} \pm 0.30\phi_{25}^{-1}\phi_{30}$	$\pi_3 \rightarrow \pi_1^*$: $C_6H_5 \rightarrow C_6H_5CON_3$, delocalized $\pi_2 \rightarrow \pi_1^*$: $C_6H_5 \rightarrow C_6H_5CON_3$, delocalized $\pi_1 \rightarrow \pi_1^*$: $CON_3 \rightarrow C_6H_5CON_3$, delocalized $\pi_1 \rightarrow \pi_2^*$: $CON_3 \rightarrow C_6H_5N_3$, delocalized	4.45	4.37
$\Psi_{\mathrm{EX\,II}} = \pm 0.63\phi_{27}^{-1}\phi_{28} \pm 0.28\phi_{27}^{-1}\phi_{30}$	$\pi_3 \rightarrow \pi_1^*$: $C_6H_5 \rightarrow C_6H_5CON_3$, delocalized $\pi_3 \rightarrow \pi_2^*$: $C_6H_5 \rightarrow C_6H_5N_3$, delocalized	4.65	4.61
$\Psi_{\mathrm{EX\,III}} = \pm 0.45\phi_{26}^{-1}\phi_{28} \pm 0.18\phi_{26}^{-1}\phi_{30} \pm 0.46\phi_{25}^{-1}\phi_{28} \pm 0.17\phi_{25}^{-1}\phi_{30}$	$\pi_2 \rightarrow \pi_1^*$: $C_6H_5 \rightarrow C_6H_5CON_3$, elocalized $\pi_2 \rightarrow \pi_2^*$: $C_6H_5 \rightarrow C_6H_5N_3$, delocalized $\pi_1 \rightarrow \pi_1^*$: $CON_3 \rightarrow C_6H_5CON_3$, delocalized $\pi_1 \rightarrow \pi_2^*$: $CON_3 \rightarrow C_6H_5N_3$, delocalized	5.00	4.92
$\Psi_{\mathrm{EX\,IV}} = \pm 0.33\phi_{26}^{-1}\phi_{28} \pm 0.41\phi_{25}^{-1}\phi_{28} \pm 0.34\phi_{25}^{-1}\phi_{30} \pm 0.24\phi_{26}^{-1}\phi_{30} \pm 0.15\phi_{27}^{-1}\phi_{28}$	$\pi_2 \rightarrow \pi_1^*$: $C_6H_5 \rightarrow C_6H_5CON_3$, delocalized $\pi_1 \rightarrow \pi_1^*$: $CON_3 \rightarrow C_6H_5CON_3$, delocalized $\pi_1 \rightarrow \pi_2^*$: $CON_3 \rightarrow C_6H_5N_3$, delocalized $\pi_2 \rightarrow \pi_2^*$: $C_6H_5 \rightarrow C_6H_5N_3$, delocalized $\pi_3 \rightarrow \pi_1^*$: $C_6H_5 \rightarrow C_6H_5CON_3$, delocalized	5.52	5.15

using the ab initio CIS as well as the semi-empirical methods AM1-CI methods. The results are given in Table 5. The AM1-CI results match nicely with the experimental values. The SCF-MO's were calculated, the weight percent of the atomic orbitals of the different chromophores in the wave functions of the three highest occupied, φ_{25}–φ_{27} (π_1–π_3), and the three lowest unoccupied, φ_{28}–φ_{30} (π_1^*, σ^* and π_2^*), molecular orbitals are given in Table 6. Excited configurations are those which result from a one-electron transition between the three highest occupied MOs and the lowest three unoccupied MOs. The CI matrix is solved, the wave functions and corresponding energies of the first four excited states are given in Table 7.

Analysis of the wave functions of the excited states is illustrative. The wave function of the first excited state, ψ_{ex1}, is built up from a linear combination of four electronic configurations, namely, $\varphi_{27}^{-1}\varphi_{28}$, $\varphi_{26}^{-1}\varphi_{28}$, $\varphi_{25}^{-1}\varphi_{28}$ and $\varphi_{25}^{-1}\,\varphi_{30}$. The first configuration is that in which an electron is transferred from molecular orbital φ_{27} (98% localized on the benzene ring) to molecular orbital φ_{28}, a de-localized orbital over the whole molecule. The same interpretation applies to the second configuration. The third configuration corresponds to an electron transition from φ_{25}, localized on the $-CON_3$ group to φ_{28}, delocalized over the whole molecule. The fourth configuration is also between delocalized molecular orbitals. Hence, one can say that electronic transitions in aroyl azides are not those of the aryl ring and or of the azide group as is the case with aryl azides. The first electronic transition of benzoyl azide, Table 7, is a $\pi \rightarrow \pi^*$ delocalized transition, the calculated transition energy, ΔE, is 4.45 eV, which corresponds nicely with the experimental one, 4.37 eV. It is evident that the spectra of aroyl azides differ basically from the spectra of aryl azides. The first electronic transition in phenyl azide is a $\sigma \rightarrow \pi^*$ transition (from the azide group to a de-

Table 8
CI wave functions of the excited states and the corresponding transition energies (ΔE) of *p*-methylbenzoyl azide

State functions	Assignment	ΔE (eV)	
		Calc.	Obs.
$\Psi_{\mathrm{EX\,I}} = \pm 0.30\phi_{30}^{-1}\phi_{31} \pm 0.53\phi_{28}^{-1}\phi_{31} \pm 0.30\phi_{28}^{-1}\phi_{33}$	$\pi_3 \rightarrow \pi_1^*$: p-$CH_3C_6H_4 \rightarrow p$-$CH_3C_6H_4CON_3$, delocalized $\pi_1 \rightarrow \pi_1^*$: $CON_3 \rightarrow p$-$CH_3C_6H_4CO\ N_3$, delocalized $\pi_1 \rightarrow \pi_2^*$: $N_3CO \rightarrow p$-$CH_3C_6H_4N_3$, delocalized	4.41	4.34
$\Psi_{\mathrm{EX\,II}} = \pm 0.46\phi_{30}^{-1}\phi_{31} \pm 0.39\phi_{30}^{-1}\phi_{33} \pm 0.33\phi_{29}^{-1}\phi_{31}$	$\pi_3 \rightarrow \pi_1^*$: p-$CH_3C_6H_4 \rightarrow p$-$CH_3C_6H_4CO\ N_3$, delocalized $\pi_3 \rightarrow \pi_2^*$: p-$CH_3C_6H_4 \rightarrow p$-$CH_3C_6H_4N_3$, delocalized $\pi_2 \rightarrow \pi_1^*$: p-$CH_3C_6H_4 \rightarrow p$-$CH_3C_6H_4CO\ N_3$, delocalized	4.59	4.51
$\Psi_{\mathrm{EX\,III}} = \pm 0.16\phi_{30}^{-1}\phi_{31} \pm 0.51\phi_{29}^{-1}\phi_{31} \pm 0.44\phi_{29}^{-1}\phi_{33}$	$\pi_3 \rightarrow \pi_1^*$: p-$CH_3C_6H_4 \rightarrow p$-$CH_3C_6H_4CO\ N_3$, delocalized $\pi_2 \rightarrow \pi_1^*$: p-$CH_3C_6H_4 \rightarrow p$-$CH_3C_6H_4CON_3$, delocalized $\pi_2 \rightarrow \pi_2^*$: p-$CH_3C_6H_4 \rightarrow p$-$CH_3C_6H_4N_3$, delocalized	4.90	4.77
$\Psi_{\mathrm{EX\,IV}} = \pm 0.33\phi_{30}^{-1}\phi_{31} \pm 0.52\phi_{30}^{-1}\phi_{33} \pm 0.30\phi_{28}^{-1}\phi_{31} \pm 0.12\phi_{28}^{-1}\phi_{33}$	$\pi_3 \rightarrow \pi_1^*$: p-$CH_3C_6H_4 \rightarrow p$-$CH_3C_6H_4CO\ N_3$, delocalized $\pi_3 \rightarrow \pi_2^*$: p-$CH_3C_6H_4 \rightarrow p$-$CH_3C_6H_4N_3$, delocalized $\pi_1 \rightarrow \pi_1^*$: $CON_3 \rightarrow p$-$CH_3C_6H_4CO\ N_3$, delocalized $\pi_1 \rightarrow \pi_2^*$: $N_3CO \rightarrow p$-$CH_3C_6H_4N_3$, delocalized	5.33	4.96

localized orbital over the whole molecule) whereas the first electronic transition in benzoyl azide is a $\pi \rightarrow \pi^*$ transition starting from a molecular orbital mainly localized over the benzene ring to a molecular orbital de[localized over the whole molecule.

A similar analysis of the wave functions of the other excite states, $\psi_{\mathrm{EX\,II}} - {}_{\mathrm{EX\,IV}}$ is given in Table 7. It is observed that the calculated four electronic transitions are $\pi \rightarrow \pi^*$ transitions. These results agree with the spectral observations, Fig. 1.

4.2.2. *p-Methylbenzoyl azide*

The optimized geometry of the molecule was calculated using ab initio RHF and DFT procedures. Results are given in Tables 3 and 4. As in the case with benzoyl azide, the C_1–C_6 bond order is 1.036 indicating an essential single bond and the absence of π conjugation between the benzene ring and the $-CON_3$ group. The C=O bond order is 1.965 indicating a true double bond character. The triple bond character between N_3–N_4 is apparent, bond order is 2.388. The bent structure of the N_3 group is clear as the bond angle $\theta(N_2\hat{N}_3N_4)$ is 175.27°.

The wave functions of the SCF-MO's were calculated, the weight percent of the coefficients of the highest three occupied molecular orbitals φ_{28}–φ_{30}, designated as π_1-π_3, and the lowest three vacant molecular orbitals φ_{31}-φ_{33}, designated π_1^*, σ^* and π_2^* are given in Table 6.

Excitation was considered for a one-electron transfer between the highest three occupied and the lowest three unoccupied molecular orbitals. The CI –matrix was solved, the state functions and the corresponding energies are given in Table 8. The correspondence between the calculated and experimental transition energies is satisfactory.

Analysis of the wave functions of the excited states indicates clearly that none of the electronic trasitions of *p*-methylbenzoyl azide is localized over any of the chromophores (aryl, aroyl or azide) of the molecule as is the case in the spectra of aryl azides. The wave function of the first excited state of *p*-methylbenzoyl azide consists of a linear combination of the configurations: $\varphi_{30}^{-1}\varphi_{31}$, $\varphi_{28}^{-1}\varphi_{31}$ and $\varphi_{28}^{-1}\varphi_{33}$ which corresponds to a π–π^* delocalized transition observed experimentally at 4.34 eV and calculated at 4.41 eV (Fig. 8).

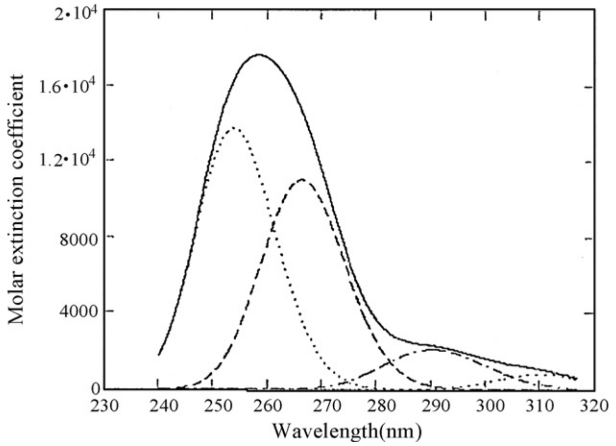

Fig. 8. Electronic absorption spectra of *p*-nitrobenzoyl azide in heptane and its Gaussian analysis.

4.2.3. *p-Methoxybenzoyl azide*

The optimized geometry is calculated, results are given in Tables 3 and 4. As is the case with the previous compounds, essential single bond exists between C_1 and C_6 (bond order is 1.096) which indicate a weak π conjugation between the aryl part and the rest of the molecule, a true double bond exists in the –C=O group, (bond order is 1.965), pronounced single bond characters exist between C(1) and N(2) and between N(2) and N(3), bond orders are 1.097 and 1.117 respectively whereas the N(3)–N(4) bond has a pronounced triple bond character (bond order is 2.385). Again, the bond angle $\theta(N\hat{N}N)$ is 175.35° indicating a slight deviation from linearity in the azide group.

Excited states were calculated, the type and composition of the three highest occupied molecular orbitals, φ_{31}–φ_{33} (π_1–π_3), and the three lowest-vacant molecular orbitals φ_{34}–φ_{36} ($\pi_1^*, \sigma^*, \pi_2^*$) are given in Table 6. Excitation is considered to occur by a one electron transfer between of the three highest occupied and any of the three lowest unoccupied molecular orbitals. The CI matrix is solved and the wave functions as well as the energies of the first four excited states are given in Table 9. It is to be noted that none of the calculated and observed transitions is an $n \rightarrow \pi^*$ transition. The correspondence between the calculated and experimental transition energies is satisfactorily.

Analysis of the form of the wave functions of the excited states is significant. The wave function of the first excited state consists of a linear combination of the following excited configurations. The configuration $\varphi_{33}^{-1}\varphi_{34}$ which represent an electron transfer from molecular orbital φ_{33}, which is extending over the $CH_3OC_6H_4$–chromophore, to the molecular orbital φ_{34} which delocalized over the whole molecule *p*-methoxybenzoyl azide. The configuration $\varphi_{33}^{-1}\varphi_{36}$ represents an electron transition between molecular oritals localized over the $CH_3OC_6H_4$ chromophore. The configuration $\varphi_{32}^{-1}\varphi_{34}$ represents an electron transition from a molecular orbital extending over the $CH_3OC_6H_4$ part of the molecule to a molecular orbital delocalized over the whole molecule *p*-methoxybenzoyl azide.

In a similar way one analyzes the wave functions of the other excited states. This analysis indicates that all the observed transitions in the electronic absorption spectrum of *para*-methoxybenzoyl azide are de-localized π–π^* transitions. This conclusion agrees with the experimental observations: weak effect of solvent polarity on band maximum (absence of contribution of charge transfer configurations to the excited states), high intensity of the observed transition (absence of n–π^* transition).

4.2.4. *p-Chlorobenzoyl azide*

The ab-initio results of the optimized geometry of the ground state are given in Tables 3 and 4. Excited states were calculated by AM1 procedure. The CI matrix of the electronic configurations which result from one electron transition between any of the three highest occupied molecular orbitals, $\varphi_{28}(\pi_1)$–$\varphi_{30}(\pi_3)$, to any of the three lowest vacant molecular orbitals $\varphi_{31}(\pi_1^*) - \varphi_{33}(\pi_2^*)$, φ_{32} is a σ^* molecular orbital, is solved. The wave functions of the excited states are given in Table 10. The results indicate that none of the observed transitions in the electronic spectrum of *p*-chlorobenzoyl azide is a

Table 9
CI wave functions of the excited states and the corresponding transition energies (ΔE) of *p*-methoxybenzoyl azide

State functions	Assignment	ΔE (eV)	
		Calc.	Obs.
$\Psi_{\mathrm{EX\,I}} = \pm 0.14\phi_{33}^{-1}\phi_{34} \pm 0.58\phi_{33}^{-1}\phi_{36} \pm 0.36\phi_{32}^{-1}\phi_{34}$	$\pi_3 \rightarrow \pi_1^*$: *p*-$CH_3OC_6H_4 \rightarrow$ *p*-$CH_3OC_6H_4CON_3$, delocalized $\pi_3 \rightarrow \pi_2^*$: Localized on *p*-$CH_3OC_6H_4$ $\pi_2 \rightarrow \pi_1^*$: *p*-$CH_3OC_6H_4 \rightarrow$ *p*-$CH_3OC_6H_4CON_3$, delocalized	4.28	4.37
$\Psi_{\mathrm{EX\,II}} = \pm 0.58\phi_{33}^{-1}\phi_{34} \pm 0.36\phi_{32}^{-1}\phi_{36} \pm 0.13\phi_{32}^{-1}\phi_{34}$	$\pi_3 \rightarrow \pi_1^*$: *p*-$CH_3OC_6H_4 \rightarrow$ *p*-$CH_3OC_6H_4CON_3$, delocalized $\pi_2 \rightarrow \pi_2^*$: Localized on *p*-$CH_3OC_6H_4$ $\pi_2 \rightarrow \pi_1^*$: *p*-$CH_3OC_6H_4 \rightarrow$ *p*-$CH_3OC_6H_4CON_3$, delocalized	4.40	4.58
$\Psi_{\mathrm{EX\,III}} = \pm 0.23\phi_{33}^{-1}\phi_{34} \pm 0.14\phi_{32}^{-1}\phi_{34} \pm 0.38\phi_{32}^{-1}\phi_{36} \pm 0.52\phi_{31}^{-1}\phi_{34}$	$\pi_3 \rightarrow \pi_1^*$: *p*-$CH_3OC_6H_4 \rightarrow$ *p*-$CH_3OC_6H_4CON_3$, delocalized $\pi_2 \rightarrow \pi_1^*$: *p*-$CH_3OC_6H_4 \rightarrow$ *p*-$CH_3OC_6H_4CON_3$, delocalized $\pi_2 \rightarrow \pi_2^*$: Localized on *p*-$CH_3OC_6H_4$ $\pi_1 \rightarrow \pi_1^*$: $CON_3 \rightarrow$ *p*-$CH_3OC_6H_4CON_3$, delocalized	5.09	4.89
$\Psi_{\mathrm{EX\,IV}} = +0.70\phi_{33}^{-1}\phi_{35} + 0.24\phi_{31}^{-1}\phi_{34} - 0.60\phi_{33}^{-1}\phi_{35} - 0.26\phi_{31}^{-1}\phi_{34}$	$\pi_2 \rightarrow \sigma^*$: CT *p*-$CH_3OC_6H_4 \rightarrow N_3$ $\pi_1 \rightarrow \pi_1^*$: $CON_3 \rightarrow$ *p*-$CH_3OC_6H_4CON_3$, delocalized $\pi_3 \rightarrow \sigma^*$: CT *p*-$CH_3OC_6H_4 \rightarrow N_3$ $\pi_1 \rightarrow \pi_1^*$: $CON_3 \rightarrow$ *p*-$CH_3OC_6H_4CON_3$, delocalized	5.53	5.61
$\Psi_{\mathrm{EX\,V}} = \pm 0.35\phi_{33}^{-1}\phi_{36} \pm 0.57\phi_{32}^{-1}\phi_{34} \pm 0.18\phi_{32}^{-1}\phi_{36}$	$\pi_3 \rightarrow \pi_2^*$: Localized on *p*-$CH_3OC_6H_4$ $\pi_2 \rightarrow \pi_1^*$: *p*-$CH_3OC_6H_4 \rightarrow$ *p*-$CH_3OC_6H_4CON_3$, delocalized $\pi_2 \rightarrow \pi_2^*$: Localized on *p*-$CH_3OC_6H_4$	5.80	5.85

Table 10
CI wave functions of the excited states and the corresponding transition energies (ΔE) of *p*-chlorobenzoyl azide

State function	Assignment	ΔE (eV)	
		Calc.	Obs.
$\Psi_{\mathrm{EX\,I}} = \pm 0.33\phi_{30}^{-1}\phi_{31} \pm 0.48\phi_{28}^{-1}\phi_{31} \pm 0.36\phi_{28}^{-1}\phi_{33}$	$\pi_3 \rightarrow \pi_1^*$: *p*-$ClC_6H_4 \rightarrow$ *p*-$ClC_6H_4CON_3$, delocalized $\pi_1 \rightarrow \pi_1^*$: $N_3CO \rightarrow$ *p*-$ClC_6H_4CON_3$, delocalized $\pi_1 \rightarrow \pi_2^*$: $N_3CO \rightarrow$ *p*-$ClC_6H_4N_3$, delocalized	4.38	4.34
$\Psi_{\mathrm{EX\,II}} = \pm 0.51\phi_{30}^{-1}\phi_{31} \pm 0.37\phi_{30}^{-1}\phi_{33} \pm 0.28\phi_{28}^{-1}\phi_{31}$	$\pi_3 \rightarrow \pi_1^*$: *p*-$ClC_6H_4 \rightarrow$ *p*-$ClC_6H_4CON_3$, delocalized $\pi_3 \rightarrow \pi_2^*$: *p*-$ClC_6H_4 \rightarrow$ *p*-$ClC_6H_4N_3$, delocalized $\pi_1 \rightarrow \pi_1^*$: $N_3CO \rightarrow$ *p*-$ClC_6H_4CON_3$, delocalized	4.58	4.53
$\Psi_{\mathrm{EX\,III}} = \pm 0.58\phi_{29}^{-1}\phi_{31} \pm 0.40\phi_{29}^{-1}\phi_{33}$	$\pi_2 \rightarrow \pi_1^*$: *p*-$ClC_6H_4 \rightarrow$ *p*-$ClC_6H_4CON_3$, delocalized $\pi_2 \rightarrow \pi_2^*$: *p*-$ClC_6H_4 \rightarrow$ *p*-$ClC_6H_4N_3$, delocalized	4.64	4.71
$\Psi_{\mathrm{EX\,IV}} = \pm 0.46\phi_{30}^{-1}\phi_{31} \pm 0.32\phi_{30}^{-1}\phi_{33} \pm 0.34\phi_{28}^{-1}\phi_{31} \pm 0.18\phi_{28}^{-1}\phi_{33}$	$\pi_3 \rightarrow \pi_1^*$: *p*-$ClC_6H_4 \rightarrow$ *p*-$ClC_6H_4CON_3$, delocalized $\pi_3 \rightarrow \pi_2^*$: *p*-$ClC_6H_4 \rightarrow$ *p*-$ClC_6H_4N_3$, delocalized $\pi_1 \rightarrow \pi_1^*$: $N_3CO \rightarrow$ *p*-$ClC_6H_4CON_3$, delocalized $\pi_1 \rightarrow \pi_2^*$: $N_3CO \rightarrow$ *p*-$ClC_6H_4N_3$, delocalized	5.28	4.92

localized or corresponds to an n → π^* transition. The correspondence between calculated and experimental transition energy is satisfactory.

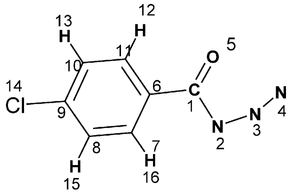

4.2.5. *p*-Nitrobenzoyl azide

The optimized geometry of *p*-NO_2 benzoyl azide has been calculated using the ab initio method and the 6-311G* basis set. The results are given in Tables 3 and 4. Some important results are evident. The calculated dipole moment is 4.26D, less than that of nitrobenzene, which indicates that the electron withdrawing effect of the $-NO_2$ group is inhibited by that of the $-CON_3$ group. The bond order between the N-atom of the $-NO_2$ group and –C of the phenyl ring is only 0.822 which indicates an essential single bond and weak π-conjunction between the nitro group and the benzene ring. The same behavior exists between C– of the benzene ring and C– of the CON $_3$ group. The bond angle $\theta(N\hat{N}N)$ is 176.16° which reflects an extent of linearity of the azide group. The partial triple bond character between the terminal adjacent nitrogen atoms and the partial double bond character between the inner nitrogen atoms are apparent, bond orders are 2.398 and 1.093, respectively.

Excited states were calculated using the AM1-procedures as was done with the previously studied compounds, results are

Table 11
CI wave functions of the excited states and the corresponding transition energies (ΔE) of *p*-nitrobenzoyl azide

State function	Assignment	ΔE (eV)	
		Calc.	Obs.
$\Psi_{\mathrm{EX\,I}} = \pm 0.50\phi_{35}^{-1}\phi_{36} \pm 0.33\phi_{35}^{-1}\phi_{38} \pm 0.20\phi_{33}^{-1}\phi_{36} \pm 0.28\phi_{33}^{-1}\phi_{38}$	$\pi_3 \rightarrow \pi_1^*$: CT $N_3 \rightarrow p$-$NO_2C_6H_4CO$ $\pi_3 \rightarrow \pi_2^*$: p-$NO_2C_6H_4CO$ $N_3 \rightarrow p$-$NO_2C_6H_4CON_3$, delocalized $\pi_1 \rightarrow \pi_1^*$: p-$NO_2C_6H_4CON_3 \rightarrow p$-$NO_2C_6H_4CO$, delocalized $\pi_1 \rightarrow \pi_2^*$: p-$NO_2C_6H_4N_3 \rightarrow p$-$NO_2C_6H_4N_3$, delocalized	4.20	4.01
$\Psi_{\mathrm{EX\,II}} = \pm 0.32\phi_{35}^{-1}\phi_{36} \pm 0.63\phi_{34}^{-1}\phi_{36}$	$\pi_3 \rightarrow \pi_1^*$: CT $N_3 \rightarrow p$-$NO_2C_6H_4CO$ $\pi_2 \rightarrow \pi_1^*$: Localized on p-$NO_2C_6H_4$	4.43	4.28
$\Psi_{\mathrm{EX\,III}} = \pm 0.33\phi_{35}^{-1}\phi_{38} \pm 0.14\phi_{34}^{-1}\phi_{38} \pm 0.59\phi_{33}^{-1}\phi_{36}$	$\pi_3 \rightarrow \pi_2^*$: p-$NO_2C_6H_4CO$ $N_3 \rightarrow p$-$NO_2C_6H_4CON_3$, delocalized $\pi_2 \rightarrow \pi_2^*$: CT p-$NO_2C_6H_4 \rightarrow CON_3$ $\pi_1 \rightarrow \pi_1^*$: p-$NO_2C_6H_4CON_3 \rightarrow p$-$NO_2C_6H_4CO$, delocalized	4.77	4.66
$\Psi_{\mathrm{EX\,IV}} = \pm 0.35\phi_{35}^{-1}\phi_{36} \pm 034\phi_{35}^{-1}\phi_{38} \pm 0.26\phi_{34}^{-1}\phi_{36} \pm 0.32\phi_{33}^{-1}\phi_{36} \pm 0.25\phi_{34}^{-1}\phi_{38}$	$\pi_3 \rightarrow \pi_1^*$: CT $N_3 \rightarrow p$-$NO_2C_6H_4CO$ $\pi_3 \rightarrow \pi_2^*$: p-$NO_2C_6H_4CON_3 \rightarrow p$-$NO_2C_6H_4CON_3$, delocalized $\pi_2 \rightarrow \pi_1^*$: Localized on p-$NO_2C_6H_4$ $\pi_1 \rightarrow \pi_1^*$: p-$NO_2C_6H_4CON_3 \rightarrow p$-$NO_2C_6H_4CO$, delocalized $\pi_2 \rightarrow \pi_2^*$: CT p-$NO_2C_6H_4 \rightarrow CON_3$	5.21	4.90

given in Table 11. The contribution of charge transfer configurations to the excited states is minor. None of the observed or calculated transitions is an n → π^* transitions.

5. Conclusions

The observed electronic absorption spectra of the studied acyl azides indicate a marked perturbation effect of the $-CON_3$ group on the energy levels of the benzene ring in spite of the fact that calculations show a minor π-conjugation between the ring and the $-CON_3$group. The observed spectra show weak solvent effect and marked band-overlap. The weak solvent effect indicates that the contribution of charge transfer configurations to the excited states is not significant. Gaussian analysis of the observed spectra indicate intense bands, a result which means the absence of n → π^* transitions.

Ab initio molecular orbital calculations give the geometry optimized values for charge density distribution, dipole moment, bond order, bond length and bond angles. The resonating forms contributing to the real structures of the molecule were predicted and pseudo-linearity of the azide group was clear. AM1-calculations give a good insight to the nature of the excited states and to the identification of the observed transitions. Calculations indicated that the electronic spectra of aroyl azides result from transitions between orbitals de-localized over the whole molecule and not between localized orbitals as is the case with aryl azides.

References

[1] I.M. Shaw, A. Talor, Can. J. Chem. 64 (1) (1986) 164.

[2] T. Zsolnai, Zentrable. Bakteriol., Parasitenk., Infektionskr. Hyg., Abt.-1: Orig., Reihe A 225 (1) (1973) 125.

[3] H. Giono, R. Camain-Giabicani, P. Giono, Bull. Mem. Fac. Mixte Med. Pharm. Dakar 11 (1963) 280.

[4] F.E. Roth, J. Schurr, E. Moutis, W.M. Govier, Arch. Intern. Pharmacodynamic 108 (1956) 473.

[5] K.R. Bhaskar, Indian J. Chem. 4 (8) (1966) 180.

[6] I. Woelfe, B. Sauerwein, T. Autrey, G.B. Schuster, Photochem. Photobiol. 44 (4) (1988) 497.

[7] C.N. Rao, R. Venkataraghavan, K.R. Bhaskar, A. Balasubramanian, Proceedings 10th international conference on spectroscopy, Maryland, U.S.A., 1962 (Spartan Press Inc., New York) 1963.

[8] V.N. Nezavibat'ko, L.N. Nikolenko, T.I. Zubareva, M.N. Semenova, Dokl. Akad. Nauk. SSSR 210 (6) (1973) 1355.

[9] A. Reisev, G. Bowes, R.J. Horne, Trans. Farad. Soc. 62 (1966) 3162.

[10] P.A.S. Smith, J.H. Hall, R.O. Kan, J. Am. Chem. Soc. 84 (1962) 485.

[11] Y.Yu. Kawa, Y. Tsuno, J. Am. Chem. Soc. 79 (1957) 5530.

[12] W.L. Butler, W. Hopkins, Photochem. Photobiol. 12 (1977) 439.

[13] T. Curtius, H. Franzen, Ber 35 (1902) 3239.

[14] C. Naegeli, A. Tyabji, L. Conrad, Helv. Chem. Acta 21 (1938) 1127.

[15] C.H. Kao, H.Y. Fang, P.P.T. Sah, J. Chin. Chem. Soc. 3 (1935) 137.

[16] T. Curtius, O. Trachmann, J. Prakt. Chem. 51 (1985) 165.

[17] M.W. Schmidt, K.K. Baldridge, J.A. Boatz, S.T. Su, T.L. Windus, M. Dupuis, J.A. Montgomery, J. Comput. Chem. 14 (1993) 1347.

[18] K. Hermansson, L. Ojamae, University of Uppsala, Institute of Chemistry, Report UUIC-B19-500 (1994).

[19] Mathcad plus 6.0, from Mathsoft© 1986–1994 Mathsoft Inc.

[20] Ya.K. Syrkin, E.A. Shott-L'vova, Dokl. Akad. Nauk S.S.S.R. 87 (1952) 639.